Optimal design of long endurance mini UAVs for atmospheric measurements.

Elkhedim Bouhoubeiny, Emmanuelle Benard, Murat Bronz, Irina Gavrilovich, Vincent Bonnin

Applied Aerodynamics Conference
Bristol, UK
19-21 July, 2016

Optimal design of long endurance mini UAVs for atmospheric measurement

E. Bouhoubeiny[†], E. Bénard[§], M. Bronz[‡], N. Gavrilović[†], V. Bonnin[†]
[†] Université de Toulouse, ISAE Dpt. of Aerodynamics, Energetics and Propulsion, 10 avenue Edouard Belin, 31400 Toulouse, France
[§] Université de Toulouse, ISAE Dpt. of Aerospace Design, 10 avenue Edouard Belin, 31400 Toulouse, France
[‡] ENAC, UAV laboratory F-31055 Toulouse, France

Abstract

The work presented in this paper is carried out under the Skyscanner project with the aim to study a fleet of coordinated mini-drones that will adaptively sample cumulus-type clouds, over periods of the order of one hour. One of the objectives of this project is to optimise the design of long endurance mini UAVs for use in atmospheric research. For that purpose, the multidisciplinary platform OpenMDAO has been used for the design and optimization procedures, aiming development of a conventional approach. Disciplinary blocks concerning aircraft dimensions, mass models and aerodynamics are implemented. This paper involves study of various optimization algorithms, including gradient-free method and genetic algorithms. The results show the efficiency of chosen methods to maximise the endurance on a given mission profile. It is shown that the flight phases defining the mission profile influence the optimal solution. The geometric parameters of the aircraft, as well as the choice of airfoil, are varied in order to investigate the overall impact on a specific mission profile. Databases of the electrical system (motor and battery) are constituted from specifications provided by the manufacturers. The performance of each pair of this database is evaluated by exploiting disciplinary blocks implemented in OpenMDAO.

1 Introduction

Unmanned Aerial Vehicles have become more popular recently as platforms for measurements of various atmospheric parameters. Indeed, the use of UAVs allows the cost-effective collection of a vast amount of scientific results [1]. However the detailed understanding of cloud dynamics requires samples that span both spatial and time scales. The Skyscanner project [2] aims to study a fleet of coordinated mini-drones that will adaptively sample cumulus-type clouds, over periods of the order of one hour. One of the objectives of this project is to optimise the design of long endurance mini UAVs for use in atmospheric research. The multidisciplinary platform OpenMDAO [3] has been used for the design and optimization.

OpenMDAO is an open source engineering analysis framework, written in Python, for analyzing and solving Multi-Disciplinary Analysis and Optimization (MDAO) problems. It provides a number of solvers and optimizers, referred to as components and drivers, which users can leverage to build new tools and processes quickly and efficiently. For this study, various disciplinary approaches are firstly implemented and defined as blocks. Secondly, the optimisation is performed with the OpenMDAO Nelder-Mead, COBYLA and NSGA2 optimizers.

A typical mission exploiting three UAVs flying simultaneously is investigated in order to serve as a basis for the design. Fig 1 displays a schematic of this mission profile. During the atmospheric measurements, each UAV will perform a specific flight phase. Consequently, we have distinguished three mission profiles:

1. UAV 3.1 maintains horizontal flight in order to locate thermals at base of the clouds.
2. UAV 3.2 conducts climb and descent cycles up to the top of the cloud and re-descends following the cloud edge. The goal is to measure the height of the cloud and follow its development.
3. UAV 3.3 performs climb and descent cycles, then it flies around the cloud and finally, it climbs to the top of the cloud before coming down, following the cloud edge.

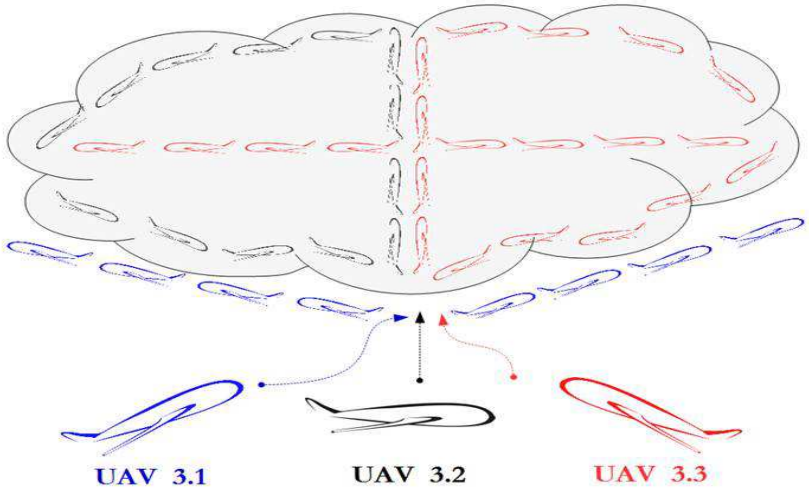

Fig 1 : Mission profile

Apart from the periods spent carrying out atmospheric measurements, the flight phases are described by climbs and descents. In order to design an individual UAV assigned to a specific measurement task, it is necessary to establish a mission profile taking into account the typical mission profiles for these measurements. Based on standard cloud characteristics and intrinsic UAV features (velocity range, turning radius ...), three nominal mission profiles without wind were established (Table 1).

Table 1: Flight phases for a defined mission

Flight phase	UAV 3.1	UAV 3.2	UAV 3.3
Climbing turns	1%	28%	23%
Climbs	11%	11%	11%
Level turns	10%	0%	2%
Level lines	65%	0%	11%
Descending turns	1%	26%	21%
Descents	11%	36%	31%
Total	100%	100%	100%

2 Optimization model

In this section, the design tool developed under the OpenMDAO platform will be presented. The principle of this optimization model is to implement the disciplinary blocks as representative of the system and which are then connected to each other by common parameters. In particular, models of geometrical sizing (aircraft

configuration), mass and aerodynamic are implemented and defined as disciplinary blocks (Fig 2). To perform the optimization, these blocks are connected in the order shown in Fig 2. Then, an optimization process can be implemented and applied to solve the optimization problem. In the following, the different disciplinary blocks are presented on 2.1, 2.2 and 2.3. The optimization processes used in this study will be presented on paragraph 2.5.

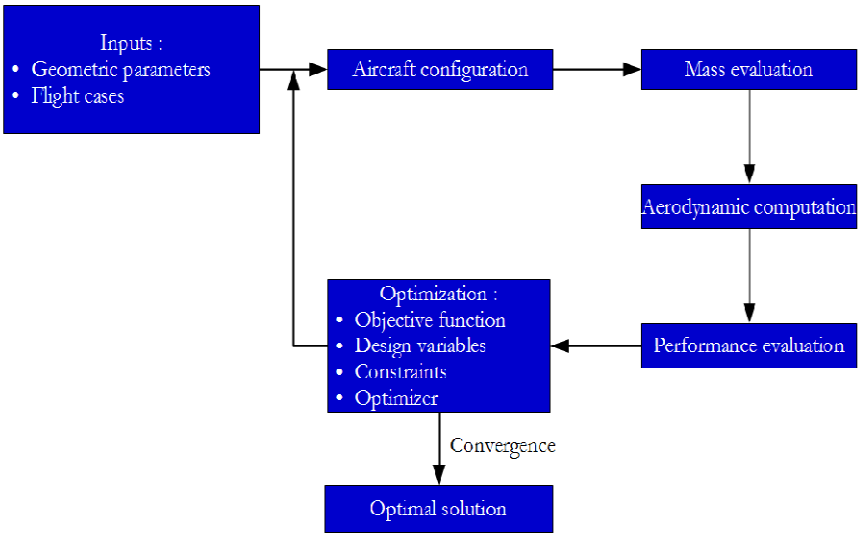

Fig 2 : Illustration of the optimization model implemented in OpenMDAO platform

2.1 Aircraft structure

The aircraft geometry block provides the characteristics (shape and size) of the body and surfaces for a selected configuration described as main variable values given as inputs. In this work, the conventional configuration has been selected. An approach allowing to relate every basic dimension of the aircraft to the given variables (span, wing area, dihedral ...) is implemented. The fuselage length is expressed in terms of the span as in the equation (1) and the maximum diameter is constant. The wings are placed in the first third of the total length of the fuselage. The horizontal and vertical tail moment arms are calculated based on conventional aircraft proportions, equation (2). In order to fix a stability criterion for the aircraft, the volume coefficients are fixed, and the required areas for vertical and horizontal tail are calculated by equations (3) and (4). Aspect ratios of the surfaces are chosen as input parameters.

$$L_{fuselage} = \frac{3}{2} C_{lht} b_{wing} \tag{1}$$

$$L_{HT} = L_{VT} = \frac{2}{3} L_{fuselage} \tag{2}$$

$$S_{vt} = C_{vt} \frac{S_{wing} b_{wing}}{L_{VT}} \tag{3}$$

$$S_{ht} = C_{ht} \frac{c_{wing} s_{wing}}{L_{HT}} \tag{4}$$

In relation to the wing geometry, the airfoils of various surfaces are fixed during iterations. The main reason for this simplification is to make the calculation faster, as scanning airfoil database and taking into account viscous effects would require significant computing time, which was beyond the scope of this paper.

In this study, three typical airfoils, shown on Fig 3, are used for the wing in order to investigate the influence of these parameters on the endurance. The airfoils "MH32", "NACA2412" are classical airfoils but the Mako airfoil refers to a flying configuration which was evaluated along the traditional configurations explored in this paper. In order to illustrate the main aerodynamic characteristics of these airfoils, the polars calculated by Xfoil for a given Reynolds number of 170000 is also shown in Fig 3. It is seen that MH32 and NACA2412 airfoils have higher endurance parameter than Mako airfoil. The effect of these airfoils on the endurance on the mission profile will be discussed in this section. The airfoil 'HT12' is chosen for horizontal and vertical tail.

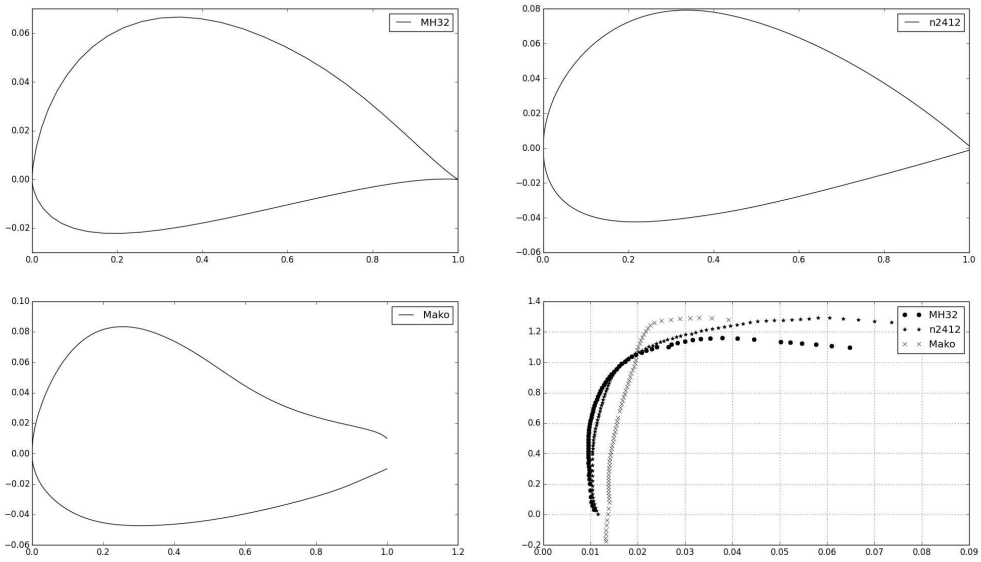

Fig 3: Candidate airfoils

In this study, the wing planform is selected to be almost elliptical with a slightly lower wing tip loading (with $c_{local} = c_{root} sin^{0.9}(y)$ chord distribution, where $y = 0: b/2$). Fig 4 and Fig 5 illustrate wing, empennage surfaces and the fuselage model.

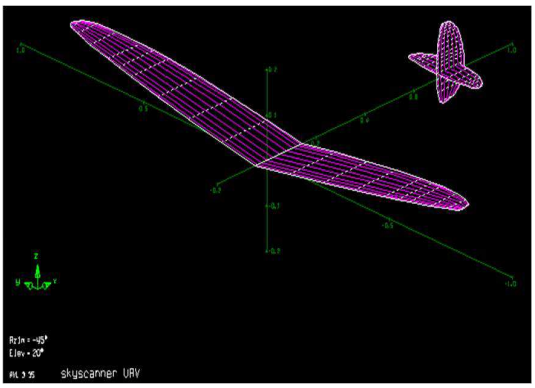

Fig 4 wing and empennage

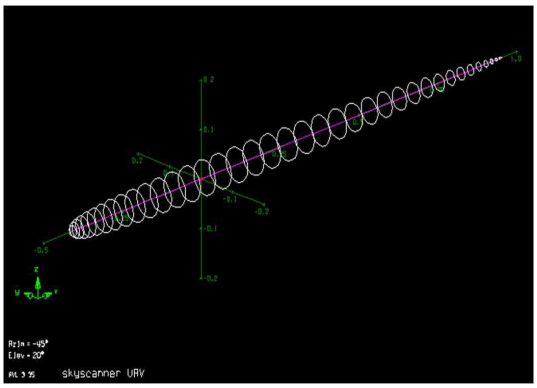

Fig 5 fuselage model

2.2 Mass model

The disciplinary block dedicated to aircraft mass consists of evaluation of the mass of each part of the structure, taking into account maximum loads acting upon it. In addition, the displacements by thickening the wings and fuselage are arbitrarily limited so that these displacements remain below 20% and 5% respectively of their length in order to limit the deformation of the UAV during the flight.

In this section, a sizing method allowing evaluating mass of structure is presented. For this aim, it is assumed that the whole structure is made of the same material, primarily carbon fiber. The fuselage is modelled as being made of two tubes: a front tube with higher diameter contains the payload and a lower diameter rear tube, supporting the empennage. The mass of each component is computed taking into account maximum loads defined as inputs. In particular, the following maximum loads have been defined to the aircraft sizing:

1. Maximum acceleration at takeoff. An acceleration of about 6 g for the catapult operation is considered.
2. Maximum cruise lift acting on the wings and empennage. For the wing, the lift applied on the wing is obtained from the lift equation multiplied by a maximal load factor. The lift on the tail is estimated on the basis of a maximum coefficient and an arbitrary never exceeded speed (NES), which are given as inputs.

$$L_{wing_{max}} = mgN_z \tag{5}$$

$$L_{ht_{maw}} = 1/2\rho\, S_{htail} NES^2 C_{l_{max}} \tag{6}$$

$$L_{vt_{maw}} = 1/2\rho\, S_{vtail} NES^2 C_{l_{max}} \tag{7}$$

3. Maximum cruise drag. The drag force applied on the wings and empennage is evaluated by a maximum drag coefficient and a never exceeded speed given in the entered parameters

$$D_{wing_{maw}} = 1/2\rho\, S_{wing} NES^2 C_{x_{max}} \tag{8}$$

4. A compressive stress induced by the difference between the thrust and the drag

The fuselage mass is evaluated taken into account loads induced by the mass of system and the lift of the empennage, combined with a criterion of maximum stress and allowable deformation. The number of carbon layers is determined thus allowing the mass budget to be computed. In order to determine the wing mass, both loads of sizing are taken into account. Firstly, the bending moment induced by the maximum acceleration during takeoff and secondly, the moment induced by the maximum lift cruise. This maximum load is estimated using a load factor of 4. The mass of the empennage is computed taking into account the aerodynamic loads acting on these surfaces. The maximum lift and drag are evaluated by using maximum coefficients given as inputs. Similarly, we calculated the mass as a function of the required thickness. Note that for the empennage, a deformation limit of 20% was applied. This mass model is compared and validated using the empirical mass model presented in [4]. Note that the system mass including all of the fixed and predefined components (autopilot, payload, servo...) of the aircraft are added to compute the total mass. To evaluate the masses of the battery and motor, both manners are chosen according to the type of optimization. In the case where an optimization process is applied, the following formula is used to add the mass of the battery:

$$m_{bat} = \frac{C_{bat} V_{bat}}{k_{bat}} \tag{9}$$

Where C_{bat} is the battery capacity and V_{bat} is the voltage. Coefficient k_{bat} is described in [4]. The motors mass is evaluated by this formula:

$$m_{motor} = P_{motor} k_{motor} \tag{10}$$

Where k_{motor} coefficient is estimated to be around 0.007.

The second method consists of exploiting motor/battery databases formed from specifications provided by the manufacturers. The description of these databases is presented in section 2.4.

2.3 Aerodynamic and endurance evaluation

The aerodynamic and flight performance block is based on a modified version of the AVL program [5] which includes the aerofoil viscous characteristics extracted from Xfoil simulations. Indeed, the wing surface is defined by a set of strip as shown in Fig 6. Each strip is described by a number of panels and located at chordwise positions. Knowing the surface area of the strip and the reference values of the aircraft, local lift, induced drag and moment coefficients can be determined. The viscous drag component is taken into account adding the corresponding airfoil drag calculated by Xfoil according to the local Reynolds number of the strip. The fuselage drag characteristics is added using a flat plate formula [4].

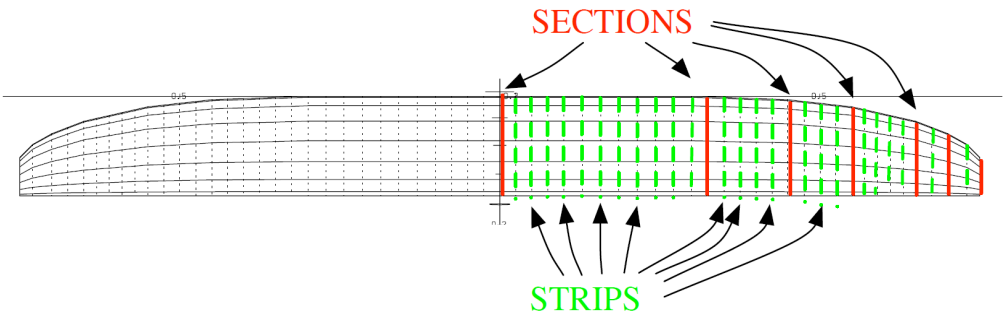

Fig 6 : section and strip description in AVL [4]

A method of evaluating the mission endurance, taking into account the distribution of different flight cases, is based on the calculation of aerodynamic power for each flight case and then determines the required electrical consummation by introducing the efficiency of the propulsion system. The aerodynamic power is evaluated as in equation (11) and electrical power in equation (12):

$$P^i_{aero} = D^i\, V_{cruise} + m_{total} g\, V^i_{vertical}, \quad for\ i = 1, \dots 6 \tag{11}$$

$$P^i_{elec} = \frac{P^i_{aero}}{\eta_{motor}\, \eta_{propeller}\, \eta_{esc}} \qquad for\ i = 1, \dots., 6 \tag{12}$$

The total electrical power for the mission profile is computed by the sum of consumption on each flight phase and taking into account the percentage which represents each phase of relative weight a_i, as exposed in Table 1. Then the endurance T is estimated from the battery capacity and the total electrical power.

$$P_{elec} = \sum_{i=1}^{6} a_i P^i_{elec} \tag{13}$$

$$T = \frac{Cap_{battery}}{P_{elec}} \tag{14}$$

2.4 Electrical system

The battery often represents one of the heaviest components of the entire vehicle. One of the most common types of batteries is the lithium polymer (LiPo), which offers a relatively high energy capacity along with low weight. Data of 140 LiPo batteries, produced by different manufacturers are presented in Fig 7. The figure shows the battery energy capacity as a function of the battery mass. A representative relation between these two parameters [11] is also shown in this figure.

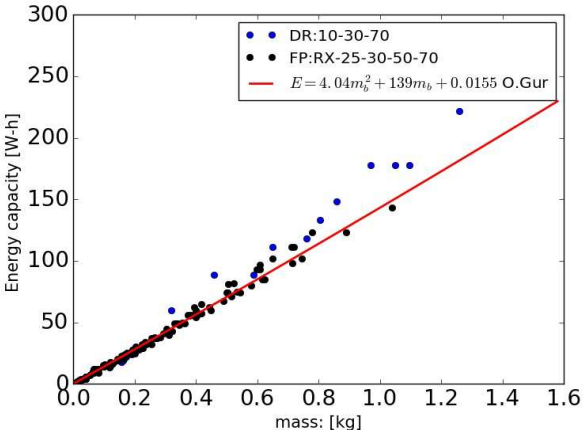

Fig 7 : Battery capacity as a function of battery mass

To constitute a motor database, the high performance AXI electric motors [7] are chosen. The manufacturer provides specifications to study more accurately the brushless motor. Fig 8 shows the maximum input power and shaft output power at maximum efficiency according to the motor mass. These results show the performance of motor are connected to its mass. The characteristics of these motors will be used in order to investigate the effect on the flight time (endurance) of the UAV.

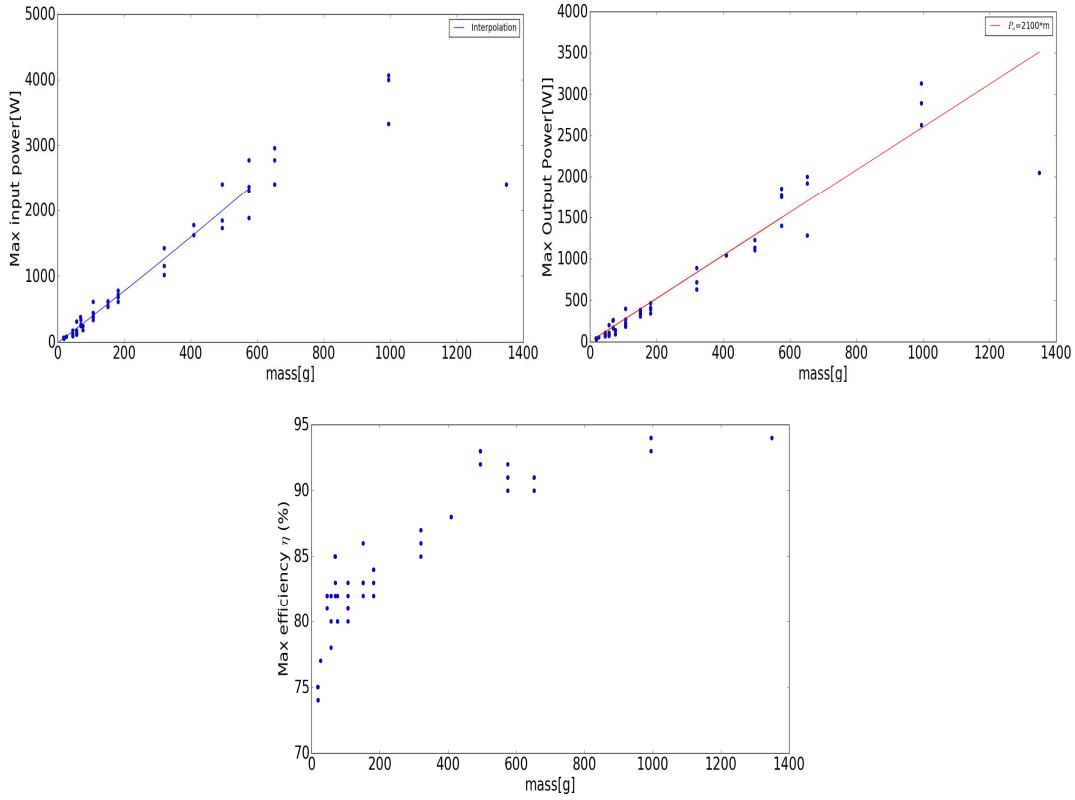

Fig 8: Top: input power as function of motor mass (left), output power as function of mass (right). Bottom: efficiency according to motor mass

2.5 Optimisation processes

The following section presents the optimisation methods which have been applied to solve the optimisation problem, which will be made explicit in section 3.

2.5.1 Nelder-Mead algorithm

The Nelder-Mead [8] method is an optimisation routine that is commonly applied as a numerical method used to find the minimum or maximum of an objective function in a multi-dimensional space. It is applied to nonlinear optimization for which derivatives may not be known. This method uses the concept of a simplex which is a special polytope of *n+1* vertices in *n* dimensions. The simplex algorithm does not need a derivative; only a numerical evaluation of the objective function is required. The basis for the simplex algorithm comes from geometry as shown in Fig 9. In three dimensional space, a simplex is a tetrahedron determined by four points (vertices) and their interconnecting line segments. At every point the objective function is evaluated. The point with the highest numerical value of all four points is perpendicularly mirrored against the opposite plain segment. This is called a reflection. The reflection can be accompanied with an expansion to take larger steps or with a contraction to shrink the simplex where an optimization valley floor is reached. The optimization procedure continues until the termination criteria are met. The termination criterion is usually the maximum number of reflections with contractions or a tolerance for optimization variables. The algorithm can be implemented in N dimensions, where simplex is a hypercube with N +1 vertex points.

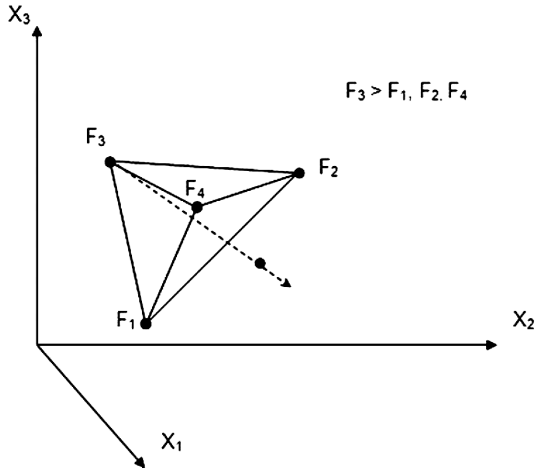

Fig 9 : Nelder-Mead simplex for three optimization parameters [8]

2.5.2 Constrained Optimisation BY linear Approximation (COBYLA)

This is an implementation of Powell's nonlinear derivative free constrained optimization that uses a linear approximation approach (Powell 1994). The algorithm is a sequential trust-region algorithm that employs linear approximations to the objective and constraint functions, where the approximations are formed by linear interpolation at (n+ 1) points in the space of the variables and tries to maintain a regular-shaped simplex over iterations.

2.5.3 Non Sorting Genetic Algorithm II (NSGA2)

The NSGA-II algorithm and its detailed implementation procedure can be found in [9]. This algorithm has been demonstrated to be among the most efficient algorithms for multi-objective optimization on a number of benchmark problems. A brief description of NSGA-II is as follows. NSGA-II uses non-dominated sorting for fitness assignments. All individuals not dominated by any other individuals are assigned front number 1. All individuals only dominated by individuals in front number 1 are assigned front number 2, and so on. Selection is made, using a tournament between two individuals. The individual with the lowest

front number is selected if the two individuals are from different fronts. The individual with the highest crowding distance is selected if they are from the same front, i.e., a higher fitness is assigned to individuals located on a sparsely populated part of the front. At each iteration new individuals (offspring) are generated. The parents also have individuals. Both these parents and offspring compete with each other for inclusion in the next iteration.

3 Analysis and results

3.1 Endurance maximisation

Main focus is to maximize the endurance corresponding to various mission profiles. For this reason, an optimization problem is formulated and solved by exploiting the disciplinary blocks previously implemented in the OpenMDAO platform. The objective function is the endurance that is computed in the performance block. The design variables include: geometrical parameters (span, wing area), operating parameter (cruise velocity) and an endurance parameter (battery capacity). Based on current regulations and field considerations, the total mass and the wingspan were defined as constraints, of less than 3 kg and less than 1.5 m, respectively. The other inputs (payloads, efficiency, airfoil geometry...) are fixed during the optimisation. Hence the optimization problem can be written as following:

$$\text{Objective: Max } Endurance$$

$$\text{Variables} : \begin{cases} lb \leq S_{wing} \leq ub \\ lb \leq b_{wing} \leq ub \\ lb \leq V \leq ub \\ lb \leq C_{battery} \leq ub \\ lb \leq m_0 \leq ub \end{cases}$$

$$\text{Constraints} : \begin{cases} Aspect\ Ratio & inequality \\ Wing\ Loading & inequality \\ m_{tot} & inequality \end{cases}$$

To solve this optimization problem, the algorithms previously presented are applied. It should be noted that the N-M and COBYLA processes are local search algorithms. During this work, it was observed that these methods converge to local optima. In order to find the global optima, numerous initializations of variables are generated and for each initialization the optimization is performed. Then the global optimal solution will be selected from lists of the local optimal. The NSGA2 algorithm is a searching global method allowing to explore efficiently the space of variables. The Fig 10 shows the convergence of these processes to the optimum solution, i.e. leading to maximum endurance. The values of variables associated with the optimal solutions are presented in the Table 2. Configuration of the optimum solution is illustrated in Fig 12. The results show that the found optimal solutions and the variable values are comparable for the different processes. Cruise velocity variation is presented in Fig 11. Consequently, the optimal solution (maximum endurance) is associated with the velocity of maximum lift-to-drag ratio.

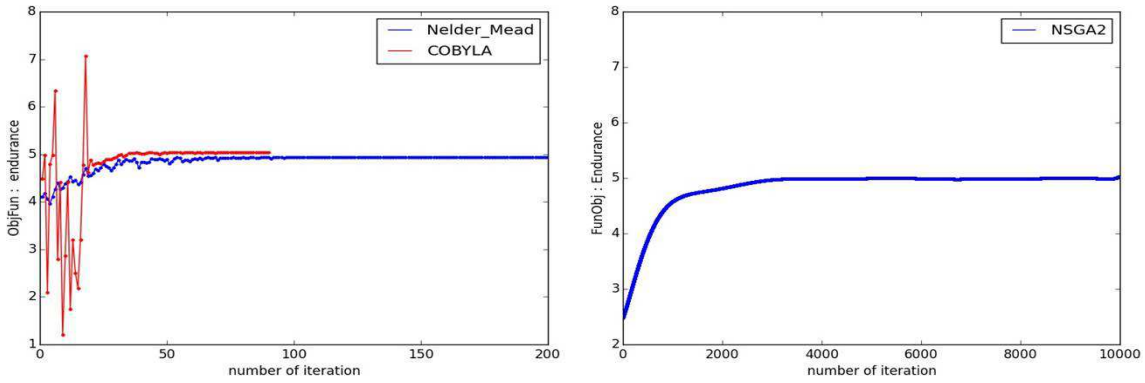

Fig 10 convergence to the optimum solution: NM and COBYLA processes (left), NSGA2 algorithm (right)

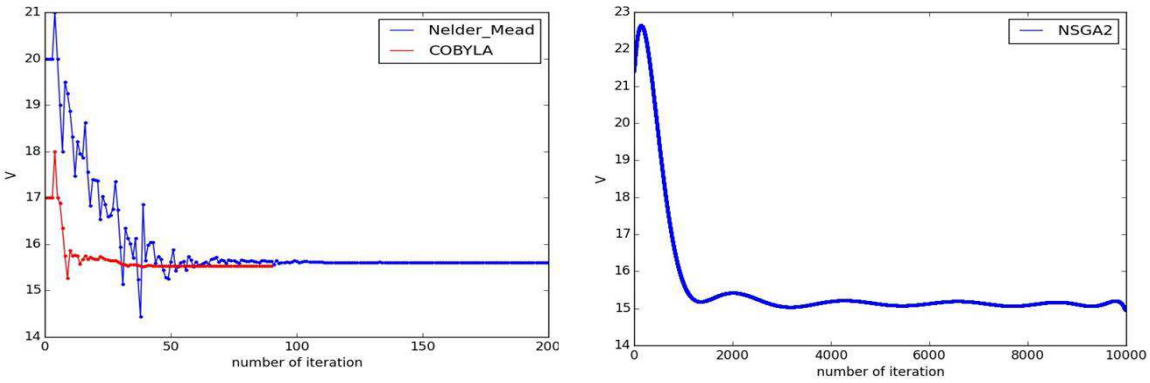

Fig 11 : variation of the velocity during optimization: NM and COBYLA (left), NSGA2 (right)

Table 2 : optimal values for the variables

variables	NSGA2	COBYLA	Nelder-Mead
$b_{wing}\ (m)$	1.44	1.44	1.37
$S_{wing}\ (m^2)$	0.17	0.18	0.16
$V\ (m/s)$	15.06	14.53	15.61
$C_{bat}\ (Ah)$	11.0	11.0	11.0

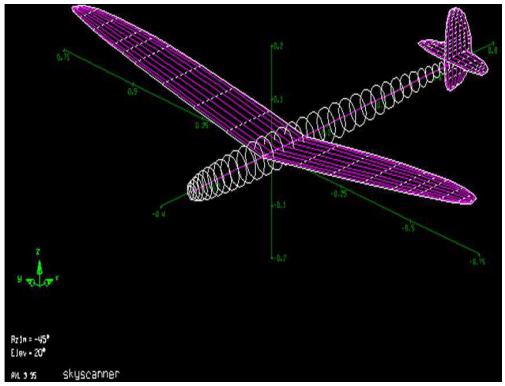

Fig 12 : configuration of the found solution

To examine the influence of the distribution of flight phases which distinguish the mission profiles, the global endurance for the three defined mission profiles is investigated using NM algorithm. As shown on Fig 13, depicting the convergence to the optimum solution for the three UAV, the endurance is affected by the distribution of flight cases. Indeed, the optimal value is higher in the case of profile mission dominated by straight lines as this flight case is related to lower power consumption, leading to more significant flying time.

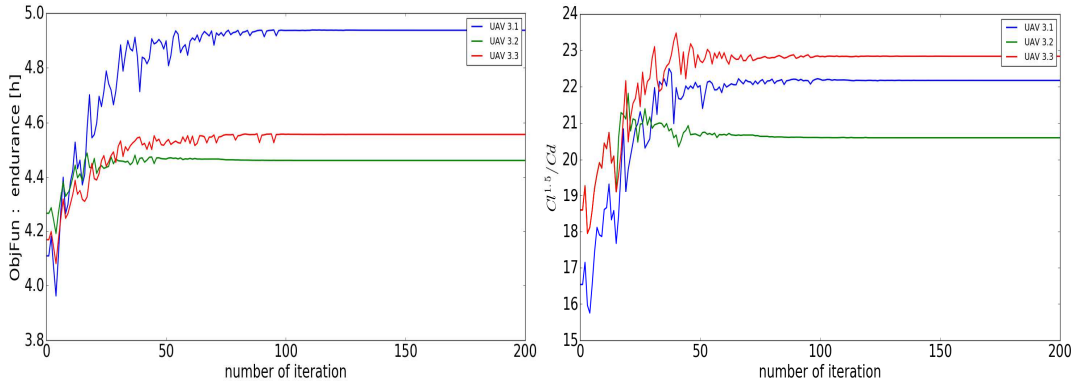

Fig 13: convergence to the optimum solution for the three mission profiles: endurance (left), variation of the lift to drag ratio (right)

The mission UAV 3.1 is chosen to investigate the effect of airfoils on the mission performance. Fig 14 gives the convergence endurance using the candidate airfoils shown on Fig 3. It is observed that the maximum endurance on the mission profile is significantly influenced by this parameter. Indeed, the optimum solutions (maximum endurance) are of 4.18, 4.78 and 4.98 hours using the airfoils of Mako, MH32 and NACA2412 respectively. To better investigate this effect of airfoils, also shows the evolution of lift and drag coefficients.

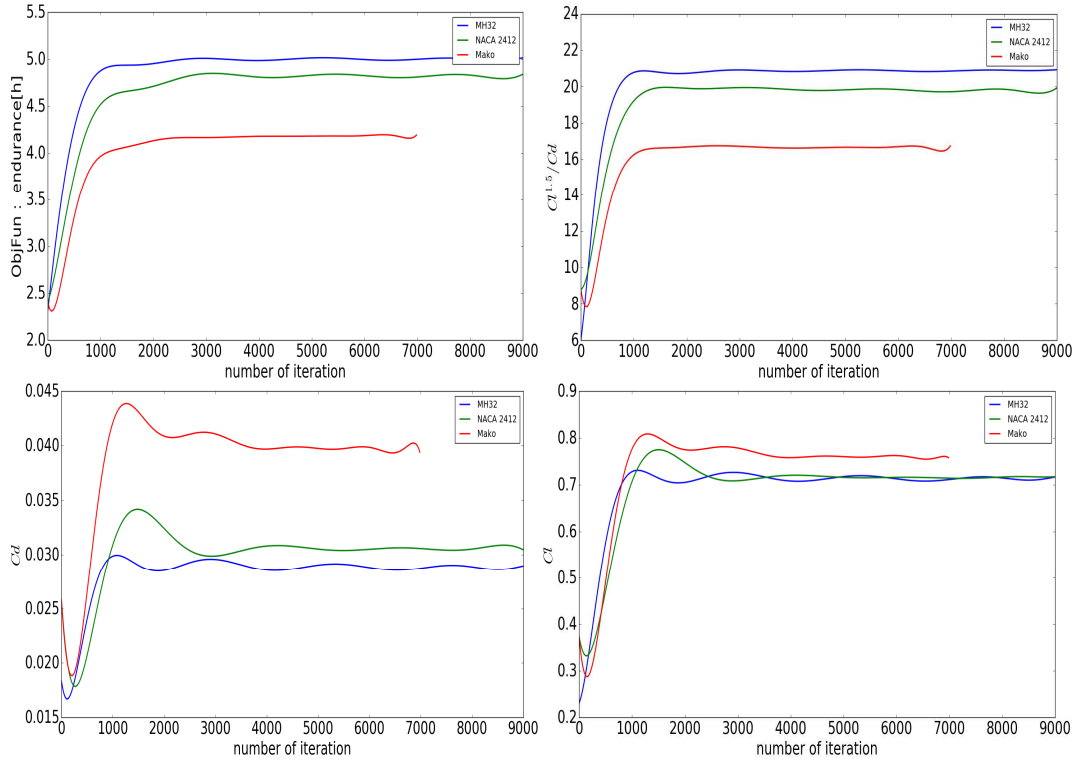

Fig 14 : Top: convergence to the optimum solution for various airfoils (left), variation of lift-drag ratio. Bottom: variation of the drag coefficient (lift) and lift coefficient (right)

These results show that the airfoil of Mako has a higher coefficient of drag than the other airfoils. Conversely, it is observed that the lift coefficient is relatively less important in the case of airfoil Mako. This means that adding the viscous drag and not induced drag, is behind the difference of endurance parameter in Fig 14. As results, usage of airfoil Mako induces a higher drag and consequently the endurance on the mission profile is less important due to consumption.

The variations of the geometrical parameters (span, and wing area), cruise velocity and the total mass are given in Fig 15. Using the airfoil of Mako, the maximum endurance is of 4 hours. This is found at $S_{wing} = 0.16m^2$, $b_{wing} = 1.35m$ with a total mass of $M_{tot} = 1.81kg$. The maximum endurance using the airfoils of MH32 and NACA 2412 are similar and they are found at $S_{wing} = 0.18m$, $b_{wing} = 1.44\ m$ with a total mass of $M_{tot} = 1.83kg$. It is seen that the optimal solutions are found at different values of the geometrical parameters.

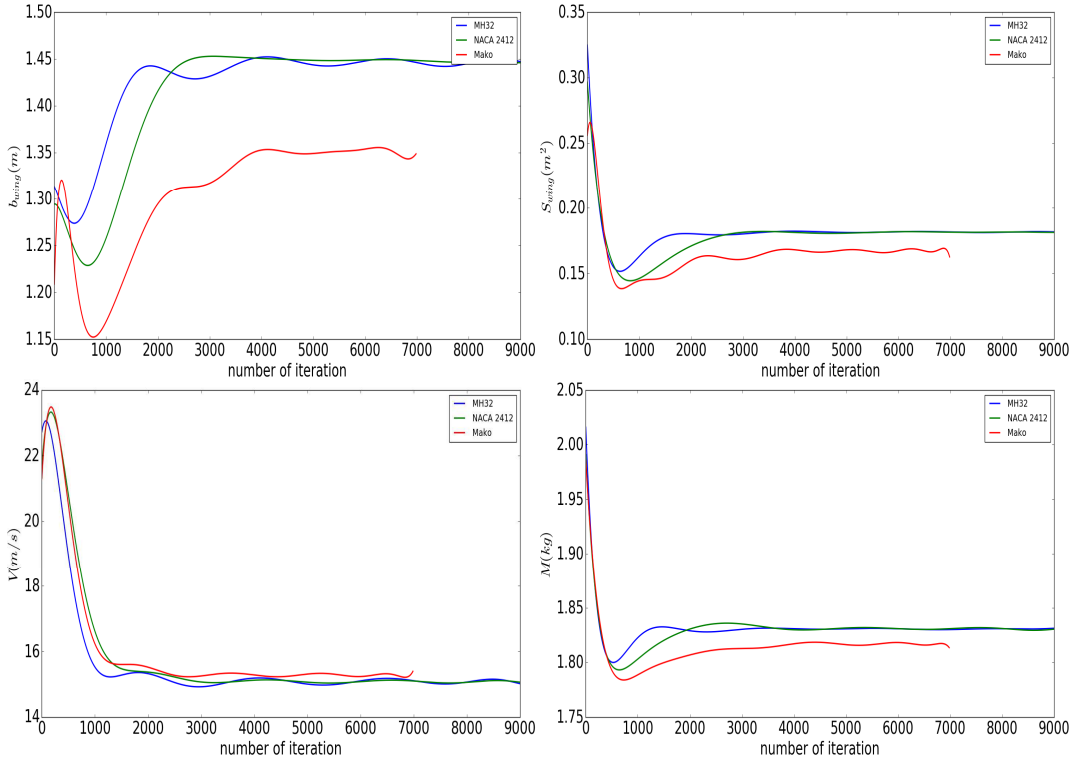

Fig 15: Top: variations of the geometrical parameters: span (left) and wing area (right). Bottom: variation of the cruise velocity (lift) and total mass (right)

3.2 Integrating the electric system

In this part, the effect of the electrical system on endurance is analysed using database of battery/motor containing characteristics of performance. The masses of the aircraft structure (fuselage, wing and empennage) and the aerodynamic coefficients are computed by the disciplinary blocks 'mass evaluation' and 'aerodynamic computation' presented on section 2, respectively. The masses of battery and motor are added from database previously presented, so, they are not fixed. The density of energy and efficiency associated at each battery/motor combination of the database was taken into account to evaluate the endurance. The optimum geometrical parameters ($S_{wing} = 0.18m$, $b_{wing} = 1.44\ m$) obtained for the UAV 3.1 is selected. The endurance is presented by equation taken from [10] assuming that the flight time is equal to the time to drain the battery.

$$Endurance = E^* \frac{\eta_{tot} Lm_{bat}}{gDm_{total} V} \tag{15}$$

For each battery/motor combination, the endurance is evaluated. The Fig 16 shows the evolution of endurance as function of the energy density for two different flight velocities. The aerodynamic coefficients are expressed as a function of the total mass. This means that the variations of the mass change the required coefficients and therefore endurance. Thus, variations in battery power and motor efficiency can impact the endurance of the UAV. Increasing the speed has an important impact on the endurance as shown in Fig 16. This is related that the high speed flight requires increase the energy expenditure.

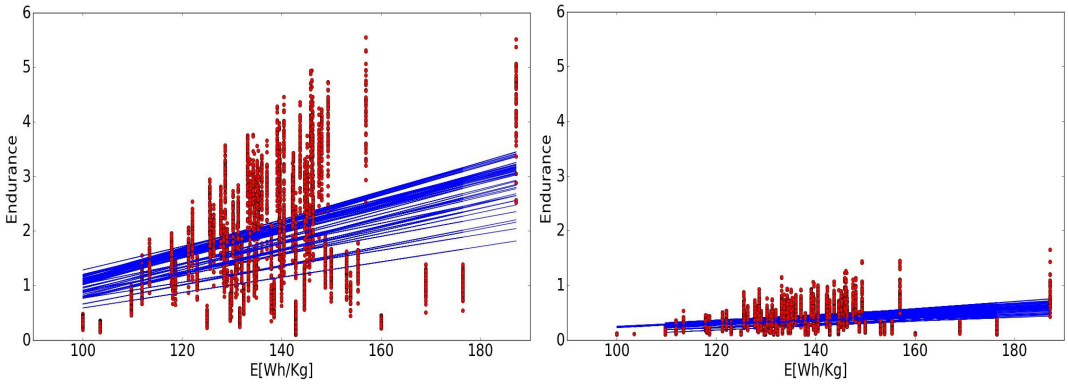

Fig 16: endurance according to mass specific energy: V= 15 m/s (left), V=30 m/s (right)

4 Conclusion

In this study, an optimization tool is presented. In order to investigate the most efficient method we study different optimization methods, their accuracy and computational time. Concerning the local search methods (N-M and COBYLA), it was shown that a multi-start (several optimizations with different initial values) is required to find the overall optimum solution. The comparison with the results of overall search method (NSAG2 process) shows the efficiency of these methods in terms of time cost. The Nelder-Mead method is chosen as candidate in order to investigate the effect of different parameters on the endurance. In particular, the evolution of the endurance as function of mission profile of UAV is investigated and shows the influence of flight phases. This is associated at the high aerodynamic coefficients which are required for some flight cases. Different airfoils are used to highlight the influence of this parameter. It is seen that this parameter significantly influences the endurance on the mission profile. It was demonstrated that the profile associated with lower endurance has greater value of viscous drag. This shows the requirement of taking into account the viscous effects for an accurate analysis. The disciplinary blocks implemented in OpenMDAO platform are used to evaluate the endurance varying the characteristics of the electrical system. The endurance for a configuration presenting optimum geometrical parameters was evaluated integrating database of the electrical system (battery and motor). For each battery/motor combination of the database, the endurance is evaluated taking into account its characteristics (mass, capacity and efficiency). Then, a ranking by flight time can be performed. Furthermore, the effect of the cruise velocity on the endurance was investigated. It was seen that the endurance on the mission profile associated of the same battery/motor combination is affected by variation of cruise velocity. This shows the effect of the aerodynamic of the UAV on the energy expenditure.

Acknowledgement

The authors would like to gratefully acknowledge the "Réseau Thématique de Recherche Avancée STAE" for its financial support during the Skyscanner project monitored by "Laboratoire d'analyse et d'architecture des systèmes de Toulouse".

REFERENCES

[1] V. Ramanathan, M. V. Ramana, G. Roberts, D. Kim, C. Corrigan, C. Chung, and D. Winker. Warming trends in asia amplified by brown cloud solar absorbation. Nature, vol. 448, no. 7153, pp. 575-578, 2007.

[2] S. Lacroix, G. Roberts, E. Benard, M. Bronz, F. Burnet, E. Bouhoubeiny, J.P Condomines, C. Doll, G. Hattenberger, F. Lamraoui, A. Renzaglia, and Ch. Reymann. Fleets of enduring drones to probe atmospheric phenomena with clouds. European Geosciences Union General Assembly 2016, Vienna (Austria), 17-22 April 2016.

[3] http://openmdao.org

[4] M. Bronz, A Contribution to the Design of Long Endurance Mini Unmanned Aerial Vehicles. PhD thesis, ISAE, 2012.

[5] M. Bronz, G. Hattenberger, and J-M. Moschetta. Development of a Long Endurance Mini-UAV: ETERNITY. IMAV 2013, International Micro Air Vehicle Conference and Flight Competition

[6] http://www.flightpower.co.uk/

[7] http://www.hobbyexpress.com/axi_motors_277_ctg.htm

[8] Nelder, J.A., and Mead, R "A simplex method for function minimization," Computer Journal, 7(4) (1965): 308-313

[9] K. Deb, A. Pratap, S. Agarwal, and T. Meyarivan, "A fast and elitist multiobjective genetic algorithm: NSGA-II," IEEE Trans. Evol. Comput. , vol. 6, no. 2, pp. 182–197, Apr. 2002.

[10] M. Hepperle. Electric flight: Potential and limitations. In AVT-209 Workshop on ENERGY EFFICIENT TECHNOLOGIES AND CONCEPTS OPERATION, October 2012.

[11] O. Gur and Aviv Rosen. "Optimizing Electric Propulsion Systems for Unmanned Aerial Vehicles", Journal of Aircraft, Vol. 46, No. 4 (2009), pp. 1340-1353.